

A new model for large landslides in sensitive clay using a fracture mechanics approach

P.E. Quinn, M.S. Diederichs, R.K. Rowe, and D.J. Hutchinson

Abstract: A new model is proposed for the development of large landslides in sensitive clay, and supported by concepts from fracture mechanics. A key assumption in this new model is that the complete failure surface develops before the onset of significant movement, thus predetermining the final extent of failure. The appearance of retrogression is actually the rearward advancing disruption of a monolithic slide mass over a growing zone of liquefied clay. It is seen that the likelihood of propagation of failure, and the resulting occurrence of a large landslide, depend primarily on the brittleness of the sensitive clay. The potential length of shear band propagation is limited by slope geometry, and increases for higher riverbanks and for flatter slopes above the riverbank. The model explains why large landslides in sensitive clay often terminate just adjacent to a reverse break in slope, such as an older landslide crater or a stream gully. The model also indicates that large landslides in sensitive clay could be expected to occur suddenly after a large single perturbation, such as an earthquake, or after a seemingly innocuous small trigger following the accumulation of a large number of annual load cycles, as observed frequently in nature.

Key words: sensitive clay, progressive failure, fracture mechanics, retrogressive landslides, brittleness.

Résumé : Un nouveau modèle est proposé pour expliquer le développement de grands glissements de terrain dans de l'argile sensible, ce modèle étant supporté par les concepts de mécanique de rupture. Une hypothèse importante de ce nouveau modèle est que la surface de rupture complète se développe avant l'apparition de mouvements significatifs, ce qui permet de prédéterminer l'ampleur finale de la rupture. L'apparence de rétrogression est en fait l'avancement vers l'arrière de la rupture d'une masse monolithique glissant sur une zone grandissante d'argile liquéfiée. Il est observé que la probabilité de propagation de rupture, et le grand glissement de terrain ainsi provoqué, dépendent principalement de la fragilité de l'argile sensible. La longueur potentielle de la propagation de la bande de cisaillement est limitée par la géométrie de la pente, et augmente dans le cas de rives élevées et de pentes plus plates au-dessus de la rive. Le modèle explique pourquoi les grands glissements de terrain dans l'argile sensible se terminent souvent juste à côté d'une cassure inverse dans la pente, comme un cratère d'un vieux glissement de terrain ou un ruisseau. Le modèle indique aussi que les grands glissements de terrain dans l'argile sensible sont susceptibles de se produire de façon soudaine suite à une grande perturbation unique, comme un séisme, ou suite à un petit déclencheur d'apparence inoffensive suivant l'accumulation de plusieurs charges cycliques annuelles, comme c'est fréquemment observé dans la nature.

Mots-clés : argile sensible, rupture progressive, mécanique de rupture, glissements de terrains rétrogressifs, fragilité.

[Traduit par la Rédaction]

Introduction

Large landslides in sensitive clay are often described as being retrogressive. This idea is embedded in the literature and in practice, having been first introduced by Bjerrum (1955). This paper proposes an alternate hypothesis that some of these large landslides begin to move after the failure surface is mostly or fully formed. The style of movement,

which has the appearance of being retrogressive, involves the rearward-advancing disruption of a slowly moving monolithic slab as it translates horizontally over a growing zone of liquefied clay. The final extent of the landslide is predetermined by the extent of the failure surface that had developed prior to the first significant movement.

This paper uses the science of fracture mechanics to illustrate this alternate mechanism as a plausible explanation for the development of these large landslides. In making this argument, the paper presents the following main ideas or concepts:

- The development of a continuous failure surface, and prior establishment of the full extent of the landslide, before significant movement of large “retrogressive” landslides in sensitive clay;
- The use of fracture mechanics principles, as first applied by Palmer and Rice (1973) for progressive landslides in London clay, to explain the development of progressive failure in sensitive clay;
- The reinterpretation of novel test data presented by Tavenas et al. (1983) to develop stress (τ) – strain (γ) and stress–

Received 13 November 2008. Accepted 7 March 2011. Published at www.nrcresearchpress.com/cgj on 29 July 2011.

P.E. Quinn. BGC Engineering Inc, Victoria, BC, Canada.

M.S. Diederichs and D.J. Hutchinson. Department of Geological Sciences and Geological Engineering, GeoEngineering Centre at Queen's-RMC, Queen's University, Kingston, ON, Canada.

R.K. Rowe. Department of Civil Engineering, GeoEngineering Centre at Queen's-RMC, Queen's University, Kingston, ON, Canada.

Corresponding author: P.E. Quinn (e-mail: pquinn@bgcengineering.ca)

displacement (δ) curves for sensitive clay connecting known small-strain behaviour with known large-strain behaviour;

- The presentation of a new definition for brittleness of sensitive clay in relation to its potential for propagation of shear bands;
- The interpretation of potential for propagation of progressive failure for a variety of sensitive clays with similar sensitivity but brittleness values ranging by two orders of magnitude; and
- The development of an analytical estimate for the potential length of large progressive landslides in sensitive clay.

This paper first describes the conceptual model and then provides supporting justification.

Mechanics of retrogressive landslides in sensitive clay: proposed model

Introduction

The most commonly accepted model for development of large landslides in sensitive clay is illustrated in Fig. 1. In this “retrogressive” model, an initial small landslide occurs at the bank of a river. This initial landslide leaves an unstable scarp, resulting in a subsequent rotational slump due to the sudden shock of the first landslide. Numerous additional rotational landslides follow until the failure has retrogressed to a stable position. This model reflects retrogressive development of the landslide, in that the failure advances retrogressively away from the bank until a stable position has been reached.

The new model takes significant inspiration from Skempton (1964, 1985), who showed that slopes comprised of brittle materials (e.g., London clay) could fail progressively, with stability controlled by residual, rather than peak, strength. It also takes inspiration from Bernander (2000) and Andresen and Jostad (2002), who showed, through analytical and numerical modelling, that progressive failure was the likely mechanism for some landslides in sensitive clay. This new model was first introduced by Quinn et al. (2007b), and is explained and supported in more detail in the present paper.

This model proposes that in many cases of large landslides in sensitive clay, development is not retrogressive, strictly speaking. The apparent retrogression is rather considered to reflect the translation, subsidence, and disruption of a slowly moving monolithic slide mass over a developing zone of liquefied clay. This developing disruption begins at the free face where there is least constraint, and advances rearward toward the ultimate headscarp. The model is described in greater detail in the following subsections.

A typical retrogressive landslide in sensitive clay is shown in Fig. 2. This landslide exhibits a typical rib and ridge “thumbprint” morphology, with alternating long darker and lighter strips of ground having been torn away from the gentle clay plains adjacent to the South Nation River, which flows from left to right in the aerial photograph. The darker strips are earth grabens (i.e., ribs), with the existing vegetation preserved on the ground surface. The lighter strips are exposed clay horsts, and are often observed as triangular ridges or pyramidal pinnacles with preserved horizontal bedding (Carson 1977). The earth ribs are often tilted, but careful examination often indicates such tilting is random, rather than consistently

back-tilting, which would be indicative of rotational failure, and is more consistent with lateral spreading.

Initial development of complete failure surface

A key component of the proposed model is that prior to any observable landslide movement, the complete failure surface is formed, thus defining the approximate location of the ultimate headscarp before any significant movement begins. This failure surface develops progressively via propagation of brittle failure. This can happen quite slowly (i.e., geological time scales) due to seasonal fluctuations in loading at the toe (e.g., erosion, river-level fluctuations, and associated rapid drawdown), causing a small increment of failure each year, or very rapidly, due to liquefaction of a silt or sand layer due to an earthquake, pile driving, blasting, or some other sudden shock. Once this failure surface has formed, the slope is marginally stable, subject to general failure following some additional small perturbation. This failure surface would be continuous, but could be a series of stepped zones passing through different brittle and (or) weak layers.

The development of the complete failure surface is illustrated conceptually in Fig. 3, which shows three potential modes of development of the complete failure surface: case 1, inward, or upward, propagation from a perturbation at the river bank; case 2, downward propagation, toward the river bank, from a load well back from the river, such as construction of a road embankment; or case 3, instantaneous development due to widespread liquefaction of a loose silt layer due to transient loading such as strong earthquake shaking.

The mechanism illustrated as case 1 is believed to be the most common for large landslides in Canadian sensitive clay, which are most often triggered by erosion (Lebuis et al. 1983) and are frequently preceded by a smaller landslide at the riverbank; however, the largest recorded landslides, including ancient landslides east of Ottawa (Aylsworth and Lawrence 2003) and landslides associated with the 1663 Charlevoix earthquake near Shawinigan (Desjardins 1980) and Saint-Jean-Vianney (Leggett and LaSalle 1978), are probably case 3 events. The type of landslide illustrated as case 2 is believed to be less common in Canada, but several large landslides of this type have been documented in Sweden (e.g., Svärta, Sköttorp, and Tuve slides, per Bernander 2000). This paper will be concerned primarily with the case 1 mechanism.

An analytical treatment of the proposed mechanical model

Introduction

In the progressive failure of overconsolidated clay slopes, the mean stress along the failure surface may be substantially lower than the peak strength of the clay. This result is possible because the clay is strain weakening, losing strength after the peak strength has been reached. Notable early researchers, including Skempton (1964) and Bishop (1968), had suggested that fracture mechanics might provide a useful framework for analysing progressive failure.

Palmer and Rice (1973) applied Rice's J integral approach (Rice 1968) to the problem of progressive failure of stiff, overconsolidated slopes in London clay. They used the path independence of the J integral to obtain solutions for fracture

Fig. 1. Traditional model for development of retrogressive landslides in sensitive clay (adapted from Bjerrum 1955).

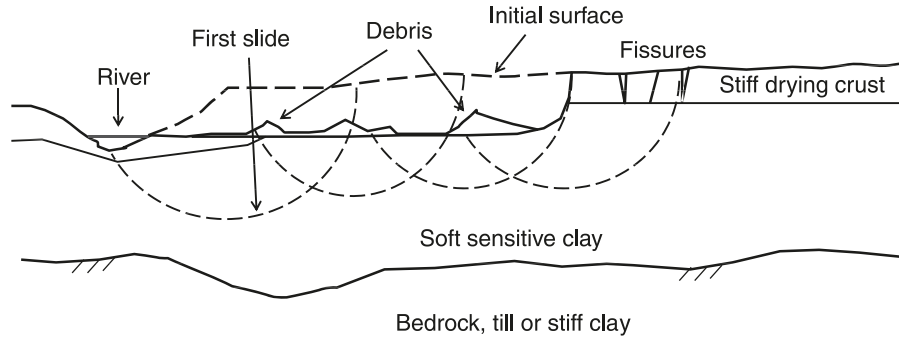


Fig. 2. Typical retrogressive landslide in sensitive clay: the South Nation River slide of 1971 (© 2008, produced under license from Her Majesty the Queen in Right of Canada, with permission of Natural Resources Canada, courtesy of the National Air Photo Library).



propagation for the case of an existing shear band of limited extent in a shear box, and for the case of a shear band propagating from a step cut into an infinite slope. This latter case approximates the conditions prior to failure in many delayed failures in London clay. A number of the more important findings from these papers are presented in the following section, where they are used to support the mechanical model previously described.

Simplified slope and behaviour along a potential failure surface

Consider an infinite slope with a step cut at the toe as illustrated in Fig. 4. One might imagine that this model approximates the long-term progressive failures in overconsolidated London clay that occur some decades after a road cut has been excavated at the toe. If the slope angle, α , is very low (e.g., 1° – 3°), then the geometry approximates that of a gently sloping clay plain adjacent to a riverbank eroded through sensitive clay in eastern Canada.

The slope consists of a strain-weakening soil with density, ρ , and peak and residual shear strengths of τ_p and τ_r , respectively. Assume that a shear band of moderate length has developed, so that shear strength has reduced to τ_r along most of its length, and there is a transition zone (“end region”) near the end of the band where shear stress ranges between

peak and residual strength. Finally, assume that this end region is small relative to the length of the band (note that the importance of this length will be examined in more detail later).

Consider three points along the potential failure surface as shown in Fig. 4: A, located well upslope of the shear band; B, located at the propagating end of the band; and C, located along the band some significant distance from its tip. At point A, shear stress and strain along the potential failure surface are, respectively,

$$[1] \quad \tau_A = \tau_g = \rho gh \sin \alpha$$

and

$$[2] \quad \gamma_A = \frac{\tau_A}{G}$$

where h is the height of the slope, and G is the shear modulus in the elastic range. Assume that the gravitational far-field shear stress, τ_A or τ_g , exceeds the residual strength, τ_r , but is less than the peak strength, τ_p . At point C on the shear band, there has been enough displacement, δ_C , along the band to reduce shear strength to the residual value, τ_r (i.e., $\delta_C \geq \delta_r$, where δ_r is the displacement required to obtain the residual strength). Shear strain in the soil above and below the shear band, where shear strains are small enough for behaviour to remain elastic, will be reduced to

$$[3] \quad \gamma_C = \frac{\tau_r}{G}$$

Figure 5 illustrates the actual and idealized stress–strain behaviour of the soil in undrained shear.

Note that behaviour is shown in terms of shear stress and strain. The concept of shear strain breaks down for the shear band, as strains are localized at some very small, undefined region. Strains become very large, perhaps approaching infinity if the localizing region is negligibly small. It is preferable to think of displacement along the shear band after it begins to form as shear stress passes the peak, and reserve the strain concept only for soil deforming in the elastic range (i.e., the soil ahead of, and above and below, the shear band). At the point of peak stress, the material behaviour must be examined from a different perspective: prior to the peak, deformations occur as finite strains in a single continuum; after the peak has been passed, and development of a shear band has initiated, it is necessary to distinguish between deformations occurring as displacements along the new discontinuity, and those occurring as strains within the two deforming continua above and below the discontinuity.

Fig. 3. Development of the continuous failure surface by different mechanisms.

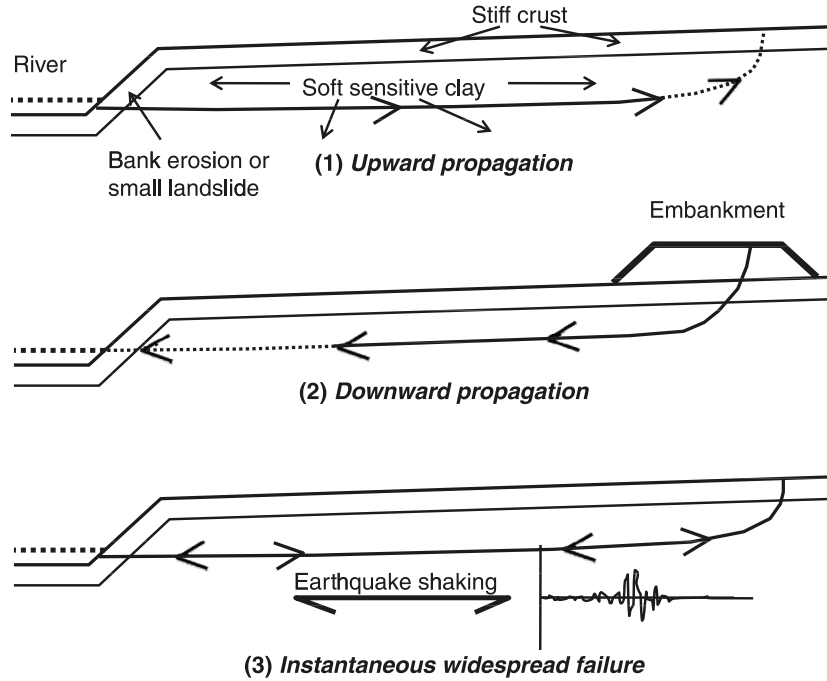


Fig. 4. Infinite slope with finite shear band (modified after Palmer and Rice 1973). A, B, C, points along potential failure surface; h , slope height; l , shear band length; α , slope angle.

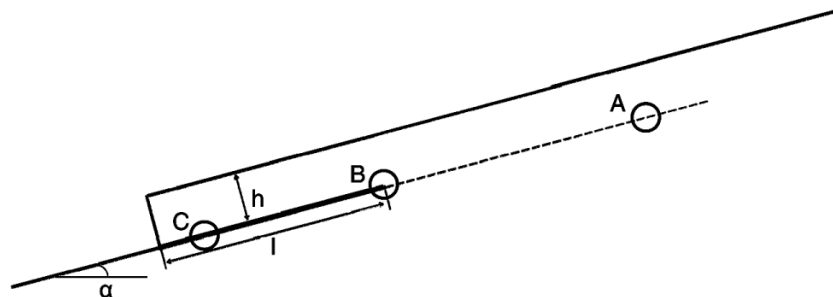
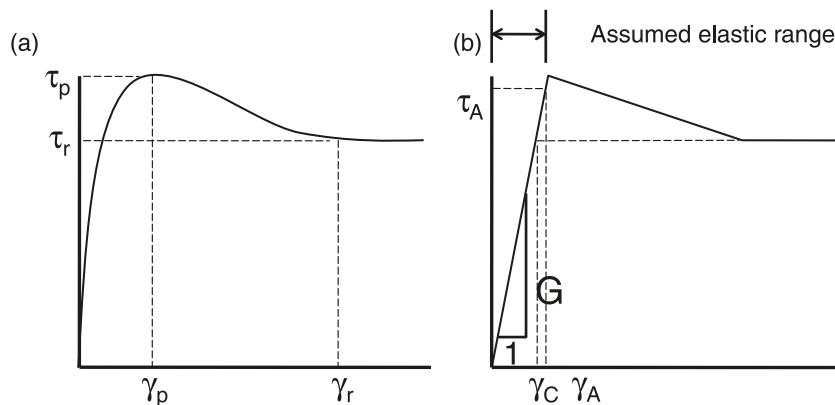


Fig. 5. Assumed stress–strain behaviour: (a) actual behaviour; (b) idealized behaviour. γ_p , shear strain at peak strength; γ_r , shear strain at residual strength.



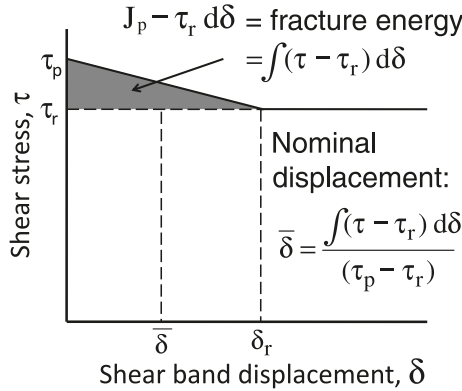
Stress–displacement behaviour of the shear band, or developing discontinuity, can be idealized as shown in Fig. 6. Stored energy becomes available on unloading to drive further fracture; this is called the fracture energy, or $(J_p - \tau_r d\delta)$, and is the shaded area above the residual strength in the unloading portion of the curve in Fig. 6. J_p is the J integral, as defined by Rice (1968).

Consider a nominal displacement, $\bar{\delta}$, defined by

$$[4] \quad \bar{\delta} = \frac{\int (\tau - \tau_r) d\delta}{(\tau_p - \tau_r)}$$

This value is some fraction of δ_r , and in the assumed idealized (linear) behaviour shown in Fig. 6, $\bar{\delta} = \delta_r/2$.

Fig. 6. Idealized stress–displacement behaviour of the shear band.



Stress–strain or stress–displacement behaviour near the tip of the shear band involves a gradual transition from the far-field conditions (i.e., τ_A and γ_A) through peak strength (and the onset of localization and slip) to the residual conditions further along the band away from its tip (i.e., τ_C , γ_r , and δ_C). Stress, strain, and displacement conditions near the band tip are as illustrated in Fig. 7, which shows the variation of shear stress, shear strain, and shear band displacement from the elastic region ahead of the band to the fully softened length of the band behind the transition area. The circled areas, identified as A, B, and C, refer to those identified in Fig. 4. Shear strain is able to decrease with shear stress as shear deformation occurs via slip along the shear band. Note that the slope has been flattened and vertical dimensions exaggerated to simplify the illustration.

If the idealized shear band stress–displacement behaviour shown in Fig. 6 is assumed, then the shear stresses in the end region, of length ω , will decrease in linear fashion behind the shear band tip as shown in Fig. 8. The length of this end region has been derived by Palmer and Rice (1973) as

$$[5] \quad \omega = \frac{9\pi}{16(1-\nu)} \frac{G}{(\tau_p - \tau_r)} \bar{\delta}$$

It will be shown that this length, ω , is a key factor in the potential for propagation of the shear band. One can see that the length of the end region depends on the elastic properties (shear stiffness, G , and Poisson’s ratio, ν), the difference between peak and residual shear strength, and the nominal displacement, $\bar{\delta}$, previously described. Since shear modulus tends to be closely related to shear strength, this equation can be rewritten as

$$[6] \quad \omega \cong 125 \frac{\tau_p}{\tau_p - \tau_r} \bar{\delta}$$

for the case of overconsolidated London clay, as estimated by Palmer and Rice (1973) from an approximation by Wroth (1972) of $G/\tau_p \cong 50$. This approximation is also reasonable for sensitive clays, which tend to fail in undrained triaxial compression at 1%–3% strain (Bjerrum 1954) or less (Vaid et al. 1979), which would yield $G/\tau_p \cong 30$ –100. This equation can be rewritten in more relevant terms for sensitive clays as follows:

Fig. 7. Shear stress, strain, and displacement conditions ahead of, near, and well behind the shear band tip.

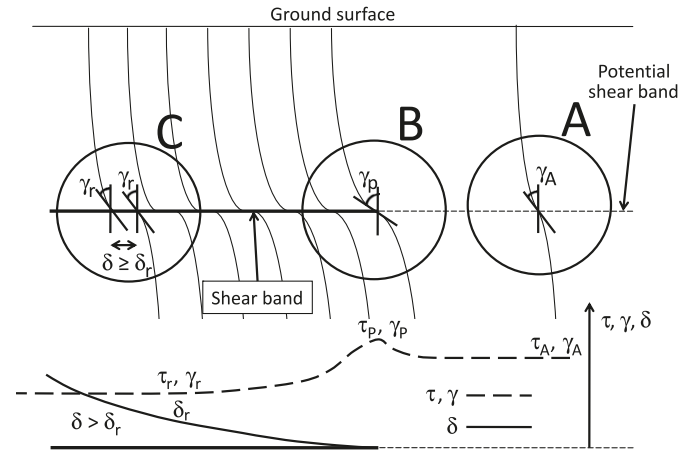
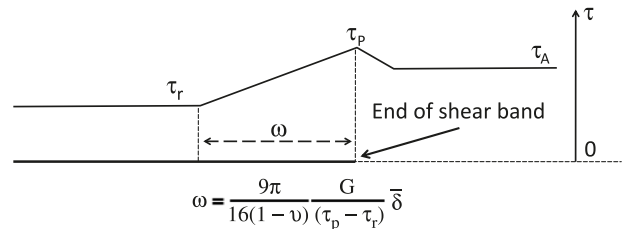


Fig. 8. Assumed stress distribution along shear band within the end region (modified from Palmer and Rice 1973). ν , Poisson’s ratio.



$$[7] \quad \omega \cong 125 \frac{S_t}{S_t - 1} \bar{\delta}$$

where S_t is sensitivity. For the soils of interest in this paper, $S_t \gg 1$, so one can approximate $\omega \cong 125\bar{\delta}$. In the case of overconsolidated London clay, $\bar{\delta} \cong 2$ –10 mm, and $S_t \cong 2$, based on results reported by Skempton (1964) and Skempton and Petley (1968), as interpreted by Palmer and Rice (1973). These values yield an end region on the order of 0.5–2.5 m. It will be seen later that the nominal displacement, $\bar{\delta}$, can be expected to vary quite substantially for different sensitive clays of similar sensitivity, yielding a wide range of potential end region lengths independent of sensitivity. This will have a marked influence on the potential for propagation of a shear band, and can be related to the brittleness of the clay.

Propagation of the failure surface

One can obtain relationships for critical conditions leading to continued propagation of a shear band, using the approach of Palmer and Rice (1973), for a slope under static loads with the geometry given in Fig. 4, as follows:

$$[8] \quad L_{cr} = \frac{\sqrt{2E'h\bar{\delta}(\tau_p - \tau_r)}}{(\tau_g - \tau_r)} - p^0 h$$

where p^0 is the initial average lateral earth pressure in the slope, over height h , before the introduction of the cut, E' is the Young’s modulus, and L_{cr} is the critical length. According to fracture mechanics principles, once the shear band reaches this length, it will propagate with no additional external load, relying on the release of internal stored energy to

Can. Geotech. J. Downloaded from www.nrcresearchpress.com by Depository Services Program on 07/30/11 For personal use only.

force the continued propagation. Termination of shear band propagation is discussed later in the paper.

Examination of this failure criterion shows that propagation is easier (i.e., the critical length needed to develop before propagation occurs is lower) for smaller values of the nominal displacement, $\bar{\delta}$, and by extension for smaller values of the end region length, ω . Readers might imagine the end region length as being representative of the sharpness of an invisible knife cutting through the clay at the end of the band. The shorter the end band, the more concentrated the source of energy being released at the end of the band upon shearing, and the sharper the imaginary knife.

Idealized stress–strain–displacement behaviour of sensitive clay

The small- to large-strain behaviour of sensitive clay may be inferred from results reported by Tavenas et al. (1983) who investigated the strain energy, w , required to remould different samples of sensitive Champlain clay. Those authors conducted four different tests on various clays, all of which had high sensitivity values (i.e., 24 to >600), and used the results to plot the reduction in shear strength with increasing strain energy. That paper used four novel test methods to estimate the energy required to remould sensitive clay samples: impact on a rigid surface; impact from falling objects; extrusion through a narrowing tube; and shearing through oscillating simple shear in a large shear box. Summary results interpreted from their paper are replotted in Fig. 9.

The samples from Saint-Thuribe and Saint-Jean-Vianney were obtained near extremely large retrogressive landslides. All of the other samples were obtained near landslides with little or no retrogression. At Saint-Léon, for example, numerous landslides had occurred in the recent past, but retrogression was generally nonexistent or very limited. These data therefore offer an opportunity to compare and contrast properties that might result in a higher potential for large retrogressive landslides.

The remoulding index, as defined by Tavenas et al. (1983), represents the percentage loss of strength from peak to remoulded, and is written as

$$[9] \quad I_r = \frac{\tau_p - \tau_x}{\tau_p - \tau_r} \times 100\%$$

where τ_x represents the strength at some given energy input, and lies between the peak and remoulded values. The strain energy, w_N , is the applied strain energy normalized by the limit state energy, w_{LS} , which is the strain energy required to reach the peak strength. Remoulding energy, w_r , is then the strain energy required to obtain the fully remoulded strength. These energy concepts are illustrated in Fig. 10.

Tavenas et al. (1983) estimated that $w_N \sim 40$ is the approximate energy released in a landslide, and interpreted remoulding index at $w_N = 40$ of the clay samples for comparison purposes. Relevant data are tabulated in Table 1. These data demonstrate that the tendency for significant retrogression (which is postulated in this paper to imply long propagation of progressive failure, and also implies a significant amount of flow) requires a very high remoulding index (which means a low remoulding energy). These data suggest that the remoulding index at $w_N = 40$ must exceed ~ 60 for large retro-

gressive landslides to occur. Stated differently, the data support the idea that a low remoulding energy is required for large retrogressive landslides to occur.

The remoulding energies at 50% strength loss (i.e., $I_r = 50\%$) are also shown in Table 1. These show that lower remoulding energies (i.e., w_N is less than 25 at $I_r = 50\%$) are associated with large landslides. There is a clear trend for lower remoulding energy to be associated with the larger retrogressive landslides.

One can use the Tavenas et al. (1983) data to interpret crude stress–strain and stress–displacement curves for the various tested clay samples. Shear stress can be interpreted directly from the remoulding index, I_r , if the peak and residual strengths are known, from

$$[10] \quad \tau_x = \tau_p - \frac{I_r(\tau_p - \tau_r)}{100\%}$$

One can then estimate the associated shear strain if certain assumptions are made. First, assume linear elastic behaviour to first yield at $\tau_p \gamma_p$. The area under the stress–strain curve to this point equals the limit state energy, and can be approximated as

$$[11] \quad w_{LS} = \frac{\tau_p \gamma_p}{2} = \frac{\tau_p^2}{2G}$$

Note that this assumes linear elastic behaviour to the point of first yield. The actual limit state energy will be somewhat higher due to nonlinearity.

One can derive the following expression for shear strain, γ_x , at any given strain energy:

$$[12] \quad \gamma_x = \frac{2w_N \times 100\%}{(\tau_{x_{i-1}} + \tau_x)} + \gamma_{x_{i-1}}$$

where i refers to the current stress–strain increment.

Strain is calculated incrementally based on the previous values of shear stress and strain, and the current values of shear stress and strain energy, where shear stress is calculated for the current value of I_r from eq. [9], and the current value of strain energy and I_r are both interpreted directly from Fig. 9. This formulation assumes a linear decrease in stress with increase in strain. The accuracy of this assumption improves as the stress increment (or incremental decrease in remoulding index) is made smaller.

The strain energy, w_N , is a multiple of w_{LS} . The peak strength of sensitive clay in triaxial compression is typically obtained at a strain of about 1%–3% (Bjerrum 1954) or less (Vaid et al. 1979 report failure in undrained triaxial compression at axial strains between 0.4 to 0.7%). Using these relationships, and assuming the limit state strain, γ_{LS} , is 1%, one can obtain stress–strain curves for the clay samples tested by Tavenas et al. (1983). A selected subset of these curves is shown in Fig. 11. Note that the cone penetrometer strengths have been used as peak strength, rather than the field vane shear strengths, but similar curves could be made based on vane strength.

If these curves are converted to stress–displacement curves, inferences can be made about the nominal displacements, $\bar{\delta}$, associated end regions, ω , and likelihood of shear band propagation. There are limited published data for large-

Fig. 9. Relationship between normalized energy and remoulding index for Champlain clay samples (replotted from Tavenas et al. 1983). w_{LS} , limit state energy.

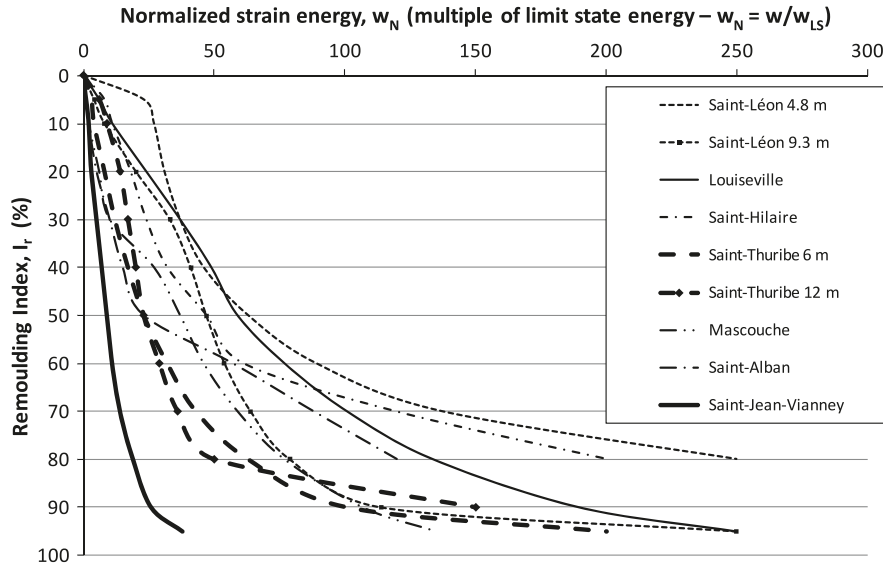
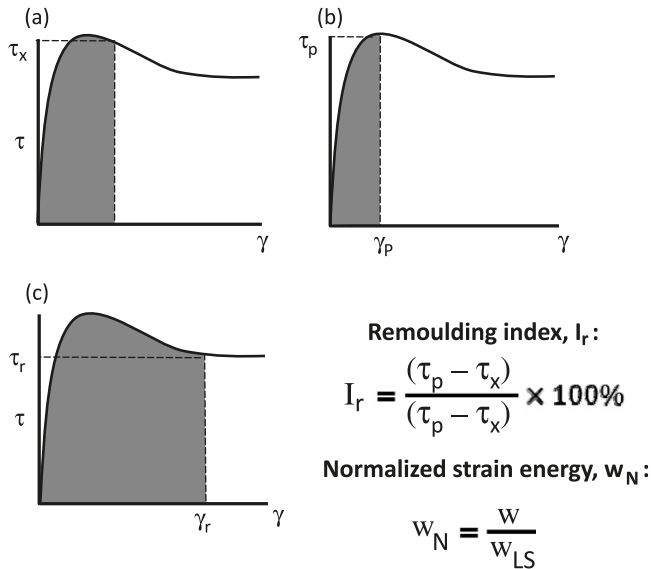


Fig. 10. Remoulding energy and remoulding index: (a) strain energy, w ; (b) limit state energy, w_{LS} ; (c) remoulding energy, w_r .



strain shear testing of sensitive clay; however, according to tests on Drammen clay by Stark and Contreras (1996), peak strength in constant-volume ring shear and direct shear testing are obtained at about 1 mm and 0.5–1 mm, respectively. It is known from Bjerrum (1954) and Vaid et al. (1979) that peak strength in undrained triaxial extension occurs at about 1%–3% axial strain, or less. While shear strain is not identical to axial strain in triaxial compression, the two measures are of the same order of magnitude, so one might conclude that a shear strain of 1%–3% is roughly equivalent to a displacement of 0.5–1 mm. If one then applies the approximate conversion that 1% strain equals ~0.375 mm displacement, the stress–displacement curve (normalized for peak strength) in Fig. 12 can be obtained.

Figure 12 has been presented primarily for illustrative purposes. Further investigation of large-strain behaviour of various sensitive clay soils would serve to improve this analysis; however, it seems reasonable to believe that the δ_r values will vary by about two orders of magnitude, as shown, for a similar group of sensitive clay samples. One would therefore expect the tendency for propagation of shear bands, and the potential for very large retrogressive landslides, to vary considerably, depending on the local nature (i.e., brittleness) of the clay.

Brittleness of sensitive clay

Bishop (1971) defined a brittleness parameter for strain-weakening materials subject to progressive failure:

$$[13] \quad I_B = \frac{\tau_p - \tau_r}{\tau_p}$$

He suggested that this parameter is important in determining the magnitude of possible error when applying limit equilibrium assumptions to the analysis of slopes that have failed progressively.

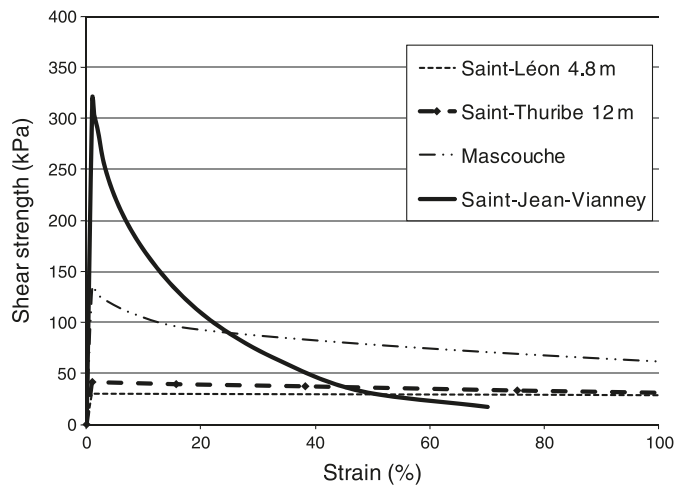
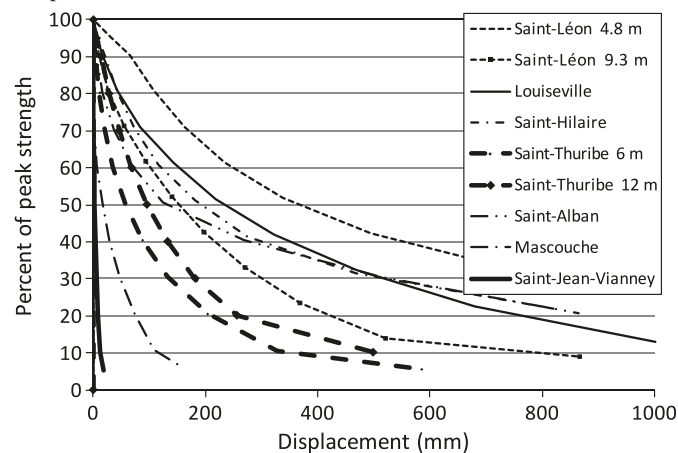
Bishop’s definition only considers the shear strength properties, and does not consider the strain, or strain energy, required to achieve the “residual” strength (which in this context, could be either the residual or remoulded strength). The preceding fracture mechanics analysis of potential for propagation of shear bands, and the data described above from Tavenas et al. (1983), both show that strain, or displacement, along the shear band is an equally important factor. A more complete definition of brittleness, for the purpose of this paper, should consider both strength values and remoulding energy. Or, more properly, it should consider both the magnitude of strength loss after peak, and the ease with which this loss is achieved. Equation [7] can be rearranged in terms of I_B and S_t to form a new brittleness parameter for sensitive clay, B_{St} :

$$[14] \quad B_{St} = \frac{1}{\omega} = \frac{I_B}{125\delta} = \frac{(S_t - 1)}{125S_t\delta}$$

Can. Geotech. J. Downloaded from www.nrcresearchpress.com by Depository Services Program on 07/30/11 For personal use only.

Table 1. Remoulding indices (at $w_N = 40$) of the clays investigated by Tavenas et al. (1983).

Site	Sensitivity (S_t)	I_r at $w_N = 40$ (%)	w_N at $I_r = 50\%$	Retrospective landslides?
Saint-Léon, 4.8 m	27	35	63	N
Saint-Léon, 9.3 m	24	39	47	N
Louiseville, 6 m	30	33	59	N
Saint-Hilaire, 5.6 m	44	46	47	N
Saint-Thuribe, 6 m	137	58	23	Y
Saint-Thuribe, 12 m	>600	74	23	Y
Mascouche, 9 m	104	54	37	N
Saint-Alban, 6.6 m	105	56	23	N
Saint-Jean-Vianney, 30 m	260	95	9	Y

Fig. 11. Stress–strain curves interpreted from Tavenas et al. (1983) for selected clay samples.**Fig. 12.** Normalized stress versus displacement for selected clay samples.

Recall that potential for propagation of a shear band increases with decreasing values of ω . The relationship for B_{St} shown in eq. [14] is thus a more useful measure of brittleness for the purpose of this paper, as it considers both the remoulding energy (indirectly, through $\bar{\delta}$) and peak and residual strength values (through I_B or S_t). The value of $1/\omega$ decreases to zero for elastic–plastic (i.e., ductile) soils, and increases to infinity for brittle soils, which have very small values of the nominal displacement, $\bar{\delta}$. Note that for very sensitive soils,

such as typical Champlain clay, $S_t \gg 1$, so $B_{St} = 1/\omega = 1/(125\bar{\delta})$, and brittleness varies inversely with the nominal displacement. For sensitive clays, therefore, brittleness tends to be a function of remoulding energy, more so than sensitivity.

This measure of brittleness has a real physical meaning in relation to the propagating shear band. Recall that ω is the length of the process zone at the end of the band where shear stress transitions from peak to residual strength (i.e., end region). It can be noted that it is also related to the width of the plastic “wake” that develops alongside a propagating crack, which is an indication of the energy lost in plastic flow, which increases with increasing ductility or toughness. The length of this process zone relates directly to the likelihood of continued propagation, as demonstrated by eq. [8]. If ω is long in relation to the shear band, then shear stresses are more or less constant along the band, and the global behaviour is ductile. If ω is short in relation to the shear band, propagation is much more likely, and global behaviour is more brittle.

Nominal displacement of sensitive clay

Approximate values of δ_r and $\bar{\delta}$ for the range of clays tested by Tavenas et al. (1983) can be interpreted from Fig. 12, as summarized in Table 2. The associated values of I_B , and resulting calculated values of ω , are also shown.

The nominal displacement, $\bar{\delta}$, determines the value of ω , since $I_B \sim 1$ for all of these very sensitive clays. The range in brittleness (or toughness) is evident in the range of calculated ω values, which vary by about two orders of magnitude for this group of otherwise similar clays. The Saint-Jean-Vianney clay is the most brittle, and Saint-Léon the least brittle, or toughest.

The physical meaning of these ω values for natural slopes in sensitive clay becomes evident when looking at eq. [8], which defines a critical length for propagation of a shear band under no load other than gravitational stresses. If there is an existing shear band with length greater than the critical length, L_{cr} , then failure is assured, since the shear band will propagate with no additional perturbation, with continued propagation driven by the release of stored energy during unloading in shear weakening.

Example of potential shear band propagation

Consider now a hypothetical example. Consider a slope similar to that illustrated in Fig. 4. Assume the height, h , to be 30 m, and the slope angle, α , to be 0.5° . Assume there is a layer that is slightly weaker and softer near the toe of the

Table 2. Nominal displacements and end region lengths for clays tested by Tavenas et al. (1983).

Site	δ_r (mm)	$\bar{\delta}$ (mm)	I_B	ω , most likely (m)	ω , range (m)
Saint-Léon. 4.8 m	>5000	1000	0.963	130	60–350
Saint-Léon. 9.3 m	~2000	400	0.958	50	25–140
Louiseville. 6 m	>3000	500	0.967	65	30–170
Saint-Hilaire	>3000	500	0.977	65	30–170
Saint-Thuribe. 6 m	~1000	200	0.993	25	10–65
Saint-Thuribe. 12 m	~1000	250	0.998	30	15–85
Mascouche. 9 m	~500	75	0.990	10	4–25
Saint-Alban. 6.6 m	>3000	500	0.990	65	30–170
Saint-Jean-Vianney. 30 m	~50	20	0.996	2.5	1–7

Note: ω values are rounded to two significant figures to reflect uncertainty in input parameters. Most likely value assumes 2% strain equals 0.75 mm displacement, which is the middle of the range of both values. The range of possible values reflects the range of possible equivalent strains (1%–3%) and displacements (0.5–1 mm) at peak strength quoted from the literature.

slope, with an undrained shear strength of 80 kPa and remoulded strength of about 1 kPa. Unit weight of the soil (ρg) is 18 kN/m³, and groundwater is located within a few metres (about 5 m) below the surface. Preconsolidation pressure is about 400 kPa at 30 m depth. These conditions could be considered fairly typical of a 30 m high riverbank carved through the gentle clay plains of southern Quebec. Further assume that $G/\tau_p \cong 50$, and Poisson's ratio, $\nu \cong 0.25$, so that $E' \cong 125\tau_p$. Also, make the assumption that the coefficient of earth pressure at rest is about 0.5. If the soil has a low remoulding energy, such that $\bar{\delta} = 0.5$ m, as in the case of the Saint-Alban clay, then one can calculate the critical length for propagation of a shear band under only gravitational stresses to be

$$[15] \quad L_{cr} = 220 \text{ m}$$

Therefore, under this geometry, with these soil conditions, if a shear band had developed to the point of being 220 m long under some process (i.e., likely involving other external loads), then at that point it would begin to propagate to failure, even if such external loads were subsequently removed.

Consider now the possibility of adding a load other than gravity. Recalling eq. [8], and noting that the term, τ_g , is meant to represent the in situ shear stress along the potential failure surface, it is clear that this stress can be higher than that solely due to gravity. Additional shear stresses could be imposed by construction of an embankment upslope, erosion of the riverbank, or by shock loads (e.g., due to explosions, earthquakes, or pile driving). This additional shear stress, if present ahead of the end of the shear band, would serve to reduce the critical length for propagation. Revised critical lengths for varying additional stresses are detailed in Table 3.

It is apparent that conditions can occur easily where the critical length for propagation becomes very short, either under a sustained load (e.g., embankment construction) or a transient load, leading to greatly increased potential for shear band propagation and general collapse. Note, however, that the shear band can propagate under these additional loads only so far as the additional driving stresses exist. Therefore, if the effects of such an external load are felt to a limited distance within the slope, then the shear band will only propagate within the limits of stress influence, and will not necessarily propagate to failure.

Table 3. Reduced critical lengths with additional driving stresses.

Additional driving stress τ_p (kPa)	Critical length (m)
0	220
10	60
20	34.5
50	15.2
100	7.9
150	5.3
200	4.0
250	3.2

Once the shear band has advanced to some degree, it becomes a weaker zone that is able to transmit stresses to its tip upon any subsequent loading increment, thus allowing the shear band to develop further upon repetitive loading. At some point, perhaps after a very large number of loading cycles, this weaker zone will have advanced to the extent where the critical length for the slope, under no external loads other than gravity, has been reached. At this point, failure is assured, and the shear band will propagate to its final extent, leading to general collapse.

Potential length of failure

Consider now the potential limits of shear band propagation, which will define the possible length of the failure surface and ultimate extent of the landslide. Given an infinite slope with a propagating shear band longer than the critical length, and uniform slope conditions, the shear band could theoretically propagate to an infinite extent as energy is continually released from the clay during strain weakening. However, the strength of the elastic slab above the shear band limits the potential propagation length. Further, variability in properties along the slope, or the existence of a significant weakness, such as a tension crack or persistent vertical joint, could force the failure to the surface.

The case of the shear band encountering an existing tension crack (or deep, open, persistent joints or fissures), resulting in sudden release of the slab, is trivial and requires no further examination. It is clear that such a scenario is possible, but it is not possible to predict the prior existence or location of

such a discontinuity. Consider instead that the elastic slab above the shear band has uniform properties and no defects. Assuming that the shear strength along the band is effectively the residual strength, τ_r , along its full length, then provided the driving stress exceeds the residual strength along the shear band, the slab will only remain in place as long as it has sufficient tensile strength (or, more properly, strength in extension) at its uppermost extent. At some point, the slab will grow to sufficient length so that the unbalanced forces along the shear band will exceed the tensile strength, and active failure will result. Figure 13 illustrates this concept.

For simplicity, assume a friction angle of 30° (reasonable for Canadian sensitive clays) and normally consolidated conditions, giving an active earth pressure coefficient of 0.33. Assume further that slope angles are very small ($<5^\circ$, for example), so that active earth pressure can be estimated based on level ground conditions.

A simple analysis of the forces acting on the slab leads to the following maximum length of the failure surface:

$$[16] \quad l = \frac{\rho gh^2}{6(\rho gh \sin\alpha - \tau_r)}$$

In the case of sensitive clay, the residual strength along the shear band is often very close to zero. One can therefore set a lower bound for length of failure to be

$$[17] \quad l = \frac{h}{6 \sin\alpha}$$

An interesting consequence is that the length of failure increases as the slope angle flattens. While this finding might at first appear counterintuitive, it is consistent with the observation of large retrogressive landslides in sensitive clay. Further, Eide and Bjerrum (1955) obtained a similar finding in their analysis of the slide at Bekkelaget. The other important consequence is that the length of failure is directly proportional to the height of the slope. This is consistent with experience of large retrogressive landslides in Canadian sensitive clay; the largest retrogressive landslides tend to occur adjacent to the highest riverbanks (e.g., Quinn et al. 2007a). This is also consistent with practical methods used to predict the maximum probable extent of retrogression adjacent to slopes, which rely in large part on slope height (e.g., Mitchell 1978).

Another interesting result emerges from careful analysis of eq. [16], which defines the maximum extent of shear band propagation based on the strength properties of the elastic slab above the band. The factor, 6, in the denominator, comes from the triangular distribution of active pressure and the earth pressure coefficient of 0.33. If the earth pressure coefficient decreases, then this factor will increase, leading to a shorter propagation length. It should be clear that if the shear band were to propagate toward a backscarp (i.e., reverse break in slope) located upslope, the active earth pressure will decrease as it approaches the change in slope. This is a consequence of decreased confinement due to the break in slope. It is therefore likely that the slab will release before the shear band reaches the break in slope, resulting in the headscarp positioning itself near to the break in slope without involving it in the failure.

This consequence of the analysis is interesting because this phenomenon is observed very frequently in the development

of large retrogressive landslides in Canadian sensitive clay. Retrogressive landslides often terminate laterally at gullies without involving the stream, and will advance near to older, surrounding retrogressive landslides without touching them, leaving an intact wall of clay — often 20 m high or more, and only a few metres wide — between the older and newer landslides. These concepts are illustrated in Fig. 14.

An example of a retrogressive landslide in sensitive clay that terminated laterally at existing gullies (i.e., the South Nation River slide of 1971) is illustrated in Fig. 2. The left and right flanks of that landslide terminated just prior to existing wooded gullies without involving them. The Lemieux slide of 1993 is similarly bounded by deep gullies along both sides. Examples of landslides terminating immediately adjacent to older landslides are documented by Hodgson (1927) for the Shawinigan Falls slide of 1924, and by Wilson and MacKay (1919) for the Saint-Thuribe slides of 1898 and 1908.

Conclusions

This paper has presented a mechanical model for the development of some “retrogressive” landslides in sensitive clay. A fundamental assumption is that the entire failure surface develops prior to first incidence of significant, noticeable movement. In other words, the landslides are not retrogressive, in the strictest sense, since the complete failure surface forms before subsequent disruption of the moving slide mass, which develops first at the free face and then moves rearward toward the ultimate headscarp, taking the appearance of retrogression by successive individual failures.

The analysis in this paper has presented mathematical support for the hypothetical mechanical model for the development of retrogressive landslides in sensitive clay. It should be noted that the time frame involved in the progressive failure will vary depending on a number of factors, including, in particular, the rheology of the geomaterials involved in the failure. Progressive landslides in overconsolidated London clay, for example, can take decades to develop, since the material is only brittle in fully drained conditions, which can take considerable time to develop. By contrast, progressive failure in sensitive clay will happen quite suddenly once conditions have been met (i.e., the critical length of the shear band has been reached), since the material is extremely brittle under undrained conditions, which requires rapid loading.

The development of the complete failure surface prior to first significant movement has been explained using concepts from fracture mechanics. The most important idea is that fracture can propagate under no additional external load in brittle materials given the right conditions. The energy released during strain weakening provides the driving impetus for continuation of fracture. If shear stress ahead of the fracture (or shear band) is adequate (i.e., higher than the residual strength, but lower than the peak strength), the failure surface can propagate progressively under no other external influence, leading to sudden, unexpected failure.

Further analysis has shown that the length of failure (e.g., ultimate size of the “retrogressive” landslide) depends on a number of factors, including slope height, residual strength, and remoulding energy of the clay (i.e., collectively, the clay’s brittleness), and the slope of the ground above the crest of the slope.

Fig. 13. Active failure of the slab above the propagating shear band. H , component of gravity force parallel to failure surface; P_a , active earth pressure; T , shear resistance along the failure surface; W , gravitational (vertical) force of the slab.

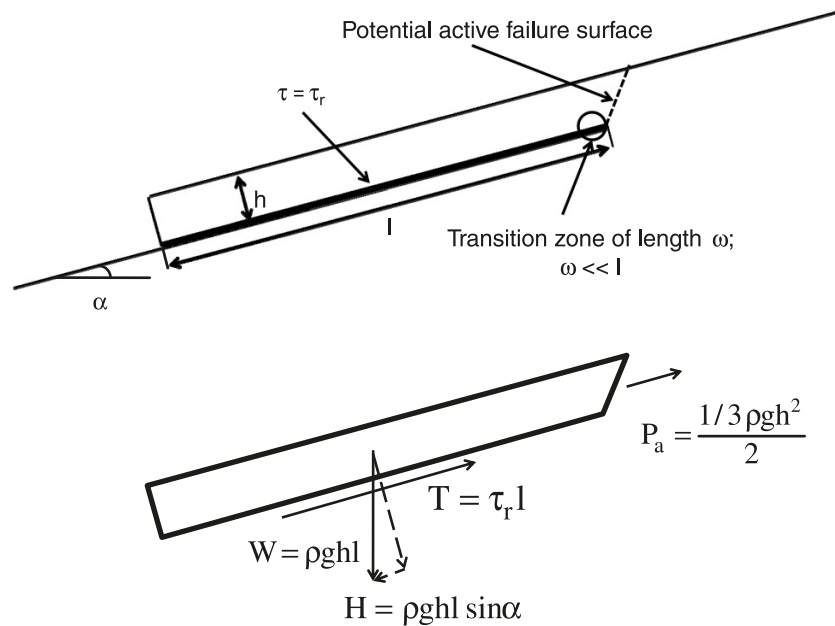
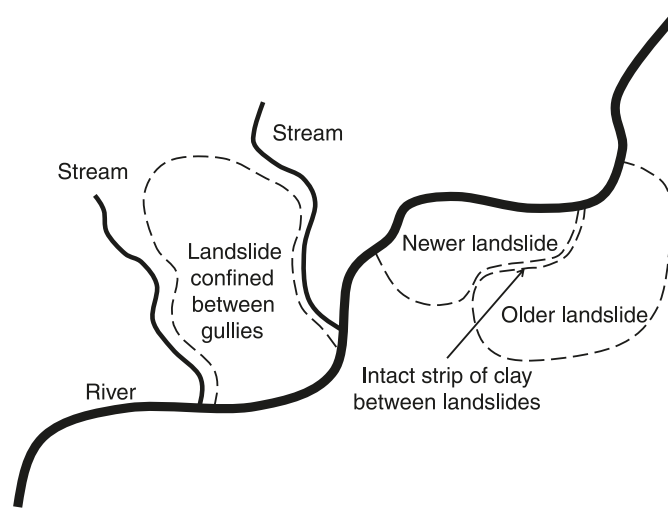


Fig. 14. Typical development of landslides near existing breaks in slope.



A number of consequences result from the proposed model. The most interesting are that the model predicts the following:

- Large landslides are more likely for more brittle clays, and less likely for tougher clays, all other properties (i.e., peak strength, sensitivity) being similar;
- Longer landslides will occur adjacent to higher riverbanks;
- Longer landslides will occur for more gently sloping ground above the riverbank crest, and shorter failure surfaces will be observed for more steeply sloping ground;
- Landslides will terminate before reaching a reverse break in slope, such as a ravine or an adjacent, older landslide crater; and
- Landslides can be initiated suddenly by a single large perturbation like an earthquake, or occur over geological time scales after a large number of annual load cycles, being triggered finally by a seemingly innocuous small perturbation.

All of these phenomena are observed frequently in nature, and are not easily explained by the more commonly accepted models for development of retrogressive landslides. Thus, it appears that this model is plausible and deserves further study.

Acknowledgements

Inspiration for the concepts in this paper came from a large number of sources in the literature, including most prominently, Skempton (1964 and 1985), Tavenas et al. (1983), Andresen and Jostad (2002), Lebuix et al. (1983), Carson (1977), Odenstad (1951), Mollard and Hughes (1973), and Bernander (2000). This work has also benefited substantially from contributions by a large number of people, who have not all necessarily agreed with the position proposed herein. The following contributed to development of ideas through discussion, which often involved lively debate: Jan Aylsworth

Can. Geotech. J. Downloaded from www.nrcresearchpress.com by Depository Services Program on 07/30/11 For personal use only.

and Didier Perret (Geological Survey of Canada), Serge Leroueil (Laval University), Marten Geertsema (BC Ministry of Forests), David Cruden (University of Alberta), Denis Demers (Quebec Ministry of Transport), Stig Bernander (private consultant, Göteborg, Sweden), Vikas Thakur and Staynor Nordal (Norwegian Technical University, Trondheim, Norway), Tore Kvalberg, Odd Gregerson, Hans Petter Jostad, Kjell Karlsrud, Lars Andresen, Kalle Kronholm, and Peter Gauer (Norwegian Geotechnical Institute, Oslo, Norway), and Dave McClung (University of British Columbia).

The first author gratefully acknowledges funding through a Natural Sciences and Engineering Research Council of Canada Postgraduate Scholarship (NSERC PGS). This work was supported financially by the Geomatics for Informed Decisions (GEOIDE) network and the Railway Ground Hazards Research Program, funded by NSERC, CN Rail, CP Rail, and Transport Canada. The work benefited substantially from the leadership and interest of Mario Ruel at CN Rail. The quality of the manuscript has also benefited substantially from contributions by two anonymous reviewers.

References

- Andresen, L., and Jostad, H.P. 2002. A constitutive model for anisotropic and strain-softening clay. *In Proceedings of the 8th International Symposium on Numerical Models in Geomechanics, NUMOG VIII, Rome, Italy, 10–12 April 2002. Edited by G.N. Pande and S. Pietruszczak.* A.A. Balkema Publishers, Rotterdam, the Netherlands. pp. 581–585.
- Aylsworth, J.M., and Lawrence, D.E. 2003. Earthquake-induced landsliding east of Ottawa: a contribution to the Ottawa Valley Landslide Project. *In Proceedings of the Third Canadian Conference on Geotechnique and Natural Hazards (Geohazards 2003), Edmonton, Alta., 9–10 June 2003. Edited by D. Das.* Canadian Geochemical Society, Edmonton, Alta. pp. 57–64.
- Bernander, S. 2000. Progressive failure in long natural slopes: formation, potential extension and configuration of finished slides in strain-softening soils. Licentiate thesis, Luleå University of Technology, Luleå, Sweden.
- Bishop, A.W. 1968. Progressive failure — with special reference to the mechanism causing it. *In Proceedings of the Geotechnical Conference, Oslo, Norway.* Norwegian Geotechnical Institute, Oslo, Norway. Vol. 2, pp. 142–150.
- Bishop, A.W. 1971. The influence of progressive failure on the choice of the method of stability analysis. *Géotechnique*, **21**(2): 168–172. doi:10.1680/geot.1971.21.2.168.
- Bjerrum, L. 1954. Geotechnical properties of Norwegian marine clays. *Géotechnique*, **4**(2): 49–69. doi:10.1680/geot.1954.4.2.49.
- Bjerrum, L. 1955. Stability of natural slopes in quick clay. *Géotechnique*, **5**(1): 101–119. doi:10.1680/geot.1955.5.1.101.
- Carson, M.A. 1977. On the retrogression of landslides in sensitive muddy sediments. *Canadian Geotechnical Journal*, **14**(4): 582–602. doi:10.1139/t77-059.
- Desjardins, R. 1980. Tremblements de terre et glissements de terrain: corrélation entre des datations au ^{14}C et des données historiques à Shawinigan, Québec. *Géographie Physique Quaternaire*, **34**(3): 359–362.
- Eide, O., and Bjerrum, L. 1955. The slide at Bekkelaget. *Géotechnique*, **5**(1): 88–100. doi:10.1680/geot.1955.5.1.88.
- Hodgson, E.A. 1927. The marine clays of eastern Canada and their relation to earthquake hazards. *The Journal of the Royal Astronomical Society of Canada.* Royal Astronomical Society of Canada, **XXI**(7): 257–264.
- Lebuis, J., Robert, J.-M., and Rissmann, P. 1983. Regional mapping of landslide hazard in Quebec. *In Proceedings of the Symposium on Slopes on Soft Clays, Linköping, Sweden, 8–10 March 1982.* Swedish Geotechnical Institute (SGI) Report No. 17, pp. 205–262.
- Legget, R.F., and LaSalle, P. 1978. Soil studies at Shipshaw, Quebec: 1941 and 1969. *Canadian Geotechnical Journal*, **15**(4): 556–564. doi:10.1139/t78-059.
- Mitchell, R.J. 1978. Earthflow terrain evaluation in Ontario. Ontario Joint Transportation and Communications Research Programme, Project Q-53, Report 213.
- Mollard, J.D., and Hughes, G.T. 1973. Earthflows in the Grondines and Trois Rivières areas, Québec: Discussion. *Canadian Geotechnical Journal*, **10**(2): 324–328. doi:10.1139/e73-029.
- Odenstad, S. 1951. The landslide at Sköttorp on the Lidán River, February 2, 1946. Royal Swedish Geotechnical Institute, Linköping, Sweden. Proceedings No. 4, pp.1–38.
- Palmer, A.C., and Rice, J.R. 1973. The growth of slip surfaces in the progressive failure of over-consolidated clay. *Proceedings of the Royal Society of London. Series A: Mathematical and Physical Sciences*, **332**(1591): 527–548. doi:10.1098/rspa.1973.0040.
- Quinn, P.E., Hutchinson, D.J., and Rowe, R.K. 2007a. Toward a risk management framework: sensitive clay landslide hazards affecting linear infrastructure in eastern Canada. *In Proceedings of the First North American Conference on Landslides: Landslides and Society, Vail, Colo., 3–8 June 2007. Edited by A.K. Turner and R.L. Schuster.* Omnipress, Madison, Wis.; Association of Environmental and Engineering Geologists, Denver, Colo. pp. 102–114.
- Quinn, P.E., Diederichs, M.D., Hutchinson, D.J., and Rowe, R.K. 2007b. An exploration of the mechanics of retrogressive landslides in sensitive clay. *In Proceedings of the 60th Canadian Geotechnical Conference and 8th Joint CGS/IAH-CNC Groundwater Conference, Ottawa, Ont., 21–24 October 2007.* Canadian Geotechnical Society (CGS), Richmond, B.C.; Canadian National Chapter of the International Association of Hydrogeologists (IAH-CNC). pp. 721–727.
- Rice, J.R. 1968. A path independent integral and the approximate analysis of strain concentration by notches and cracks. *Journal of Applied Mechanics*, **35**: 379–386.
- Skempton, A.W. 1964. Long-term stability of clay slopes. *Géotechnique*, **14**(2): 77–102. doi:10.1680/geot.1964.14.2.77.
- Skempton, A.W. 1985. Residual strength of clays in landslides, folded strata and the laboratory. *Géotechnique*, **35**(1): 3–18. doi:10.1680/geot.1985.35.1.3.
- Skempton, A.W., and Petley, D.J. 1968. The strength along structural discontinuities in stiff clays. *In Proceedings of the Geotechnical Conference, Oslo, Norway.* Norwegian Geotechnical Institute, Oslo, Norway. Vol. 2, pp. 29–46.
- Stark, T., and Contreras, I.A. 1996. Constant volume ring shear apparatus. *Geotechnical Testing Journal*, **19**(1): 3–11. doi:10.1520/GTJ11402J.
- Tavenas, F., Flon, P., Leroueil, S., and Lebuis, J. 1983. Remolding energy and risk of slide retrogression in sensitive clays. *In Proceedings of the Symposium on Slopes on Soft Clays, Linköping, Sweden, 8–10 March 1982.* Swedish Geotechnical Institute (SGI) Report No. 17, pp. 423–454.
- Vaid, Y.P., Robertson, P.K., and Campanella, R.G. 1979. Strain rate behaviour of Saint-Jean-Vianney clay. *Canadian Geotechnical Journal*, **16**(1): 34–42. doi:10.1139/t79-004.
- Wilson, M.E., and MacKay, B.R. 1919. Landslide adjacent to Rivière Blanche, St. Thuribe, Parish of St. Casimir, Portneuf County, Que. *In Report on Mining Operations in the Province of Quebec during 1918, Quebec Bureau of Mining Annual Report 1918,* pp. 152–156.
- Wroth, C.P. 1972. Stress–strain behaviour of soils. *Edited by R.H.G. Parry.* Foulis, Henley-on-Thames, UK. pp. 347–361.